Nonlinear Dynamics of Ship Steering Behaviour Under Environmental Excitations

Kostas J. Spyrou[1] and Ioannis G. Tigkas[1]

National Technical University of Athens, 9 Iroon Polytechneiou, Zographou, Athens 15773, Greece k.spyrou@central.ntua.gr

1 Introduction

Theoretical investigations on the effect of wind on ship manoeuvring and course-keeping can be traced back to the days of wind sailing [1]. In the modern period the theme continued to attract attention due to its significance for ships that are characterised either by a high superstructure or by a substantial variation of their windage area between the full-load and ballast condition [2], [3], [4], [5], [6] and [7]. Especially when operating in or near restricted waters, wind loading could bear detrimental effects for ship safety. Nonetheless, one feels that deeper understanding about the nature of phenomena that determine the course stability and turning performance of ships, even in our days, is incomplete. From this perspective, in this paper will be presented some of our key research findings concerning the "horizontal-plane" nonlinear dynamics of a modern ferry subjected to strong unidirectional wind. In such an environment, deflection of the rudder serves dual purpose: either for setting the ship on turning motion; or for offsetting the wind effect so that a desired straight-line course is maintained. Knowledge of the domains of these principal types or response in state/parameter space and the possibility some conditions to play host to more complex types of behaviour is essential for eliciting the operational profile of the ship.
A mathematical model was thus built by combining a detailed wind loading module with a standard hydrodynamic model of ship surge, sway, yaw and roll motions [8]. Course-keeping capability for any possible heading relatively to the wind was assessed firstly, by coupling the mathematical model with a well-known continuation algorithm. The stationary states that correspond to operation of the ship at specific headings were found to undergo stability changes: at saddle-nodes near to the beam wind condition; and at supercritical Hopf points that arise in head wind and lead to parasitic oscillatory yawing where the course is maintained in the mean. It was discovered that a "Bogdanov-Takens" phenomenon determines the highest wind velocity where the Hopf bifurcation can arise. Continuation of oscillatory yawing was

E. Kreuzer (ed.), *IUTAM Symposium on Fluid-Structure Interaction in Ocean Engineering*, © Springer Science+Business Media B.V. 2008

also pursued, which however was sometimes terminated by the abrupt dissapearance of the oscillations. A homoclinic bifurcation was revealed to dictate the ending of oscillations in these cases. Notably, the oscilations could have been removed in the first place by means of suitable rudder control [8]. In a parallel line of research, the evolution of ordinary turning (periodic type) responses in wind was tackled. It is known that ships may not be able to execute complete turning manoeuvres in strong wind. Continuation of these principal periodic responses revealed that this limit is determined in most cases by a homoclinic-to-saddle node phenomenon and in fewer cases by a standard homoclinic saddle connection. In either scenario, the collision with the "course-keeping" equilibria provides the critical condition. This interesting interaction is shown on a common diagram collecting the evolution of both "turning" and "course-keeping" responses.

2 Mathematical model

The mathematical model is built by superposition of a wind-loading module to a standard semi-empirical model of still-water hydrodynamics addressing the combination of ship, propeller and rudder. With the wind assumed steady and memory effects neglected, it is straightforward to turn it into a system of ordinary differential equations of the canonical autonomous form: $\dot{\mathbf{z}} = \mathbf{F}(\mathbf{z}; \mathbf{a})$
The mathematical model was inserted into MATCONT [9], a well known software for continuation analysis of dynamical systems that exploits the strengths (and weaknesses) of the MATLAB environment.
The ship examined is a modern Ro-Pax ferry with length 191.85 m, breadth 25 m, draught 6.2 m and a superstructure reaching 24 m above sea-level. The design of the ship was accomplished in the 90's during a nationally funded research project. Two propellers are able to thrust the ship to a 28 knots service speed and two rudders behind them provide sufficient steering capability. A rendered view of the ship is shown in Fig. 1.

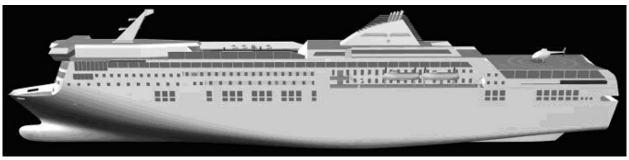

Fig. 1. The investigated Ro-Pax

Surge, sway, yaw and roll motions are considered, with essential couplings and nonlinearities included. With reference to a non-inertial system of axes whose origin is placed at midships, the equations of motion can be expressed as follows (key symbols are collected in the nomenclature):

$$\begin{aligned} Surge:\ m(\dot{u}-rv) &= X_H + X_P + X_R + X_W \\ Sway:\ m(\dot{v}+ru) &= Y_H + Y_P + Y_R + Y_W \\ Yaw:\ I_{zz}\dot{r} &= N_H + N_P + N_R + N_W \\ Roll:\ I_{xx}\dot{p} &= K_H + K_P + K_R + K_W \end{aligned} \tag{1}$$

Terms of hydrodynamic hull reaction type are approximated by Taylor-series expansions of the total (potential plus viscous) forces and moments according to standard (semi-empirical) practice in ship manoeuvring theory (e.g. [10]). The expressions can be found in Spyrou et al. [8]. Longitudinal thrust as function of propeller's rate of rotation is approximated by a polynomial fit to available propeller performance data. Rudder forces and moments are calculated as follows:

$$\begin{aligned} X_R &= -F_N \sin\delta \\ Y_R &= -(1+\alpha_H)F_N \cos\delta \\ N_R &= -\left[1+\alpha_H(x_H/x_R)\right] z_R F_N \cos\delta \\ K_R &= -(1+\alpha_H) z_R F_N \cos\delta \end{aligned} \tag{2}$$

The so-called rudder normal force F_N is determined from the well-known expression:

$$F_N = \frac{1}{2}\rho A_R U_R^2 f(\Lambda) \sin\alpha_R \tag{3}$$

Wind loads were determined according to the model of Blendermann [11] and [12], with some modification accounting for the effect of the heel angle:

$$\begin{aligned} X_W &= C_X \cdot q_{ref} \cdot A_F \\ Y_W &= C_Y \cdot q_{ref} \cdot A_L \\ N_W &= C_N \cdot q_{ref} \cdot A_L \cdot L_{OA} \\ K_W &= C_K \cdot q_{ref} \cdot A_L \cdot \overline{H} \cdot \cos^2\phi \end{aligned} \tag{4}$$

Wind loading coefficients for the different modes of motion are used assuming uniform flow. However, the wind gradient above water is taken into account. The wind loading coefficients for a passenger ship with profile similar to our investigated ship were extracted from Blendermann [12]. These coefficients were approximated by Fourier series. Both "extracted" and fitted coefficients of the investigated ferry for the four directions of motion are shown in Fig. 2.

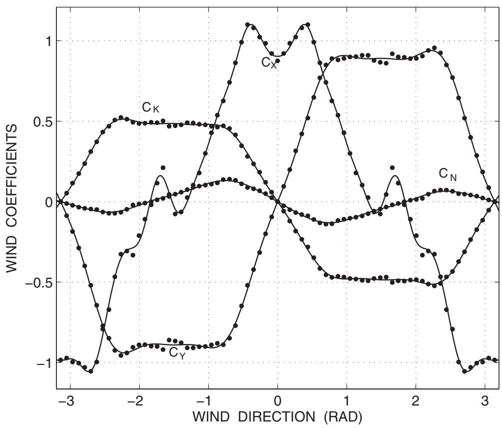

Fig. 2. Experimental and "fitted" wind loading coefficients

3 Course-keeping capability

3.1 Stationary Responses

Curves of equilibrium heading as the rudder angle is varied are shown in Fig. 3 for several wind velocities (ship velocity is fixed at the relatively low value of $U_S = 6.18$ m/s). Strong stern quartering wind causes saddle-type instability. Maximum rudder angle requirements for course-keeping are met in nearly beam wind. In wind from the bow the ship regains course stability; but in a narrow region around exact head wind the ship experiences either saddle-type unstable behaviour once more; or an oscillatory periodic yawing behaviour around the desired heading that is generated through a supercritical Hopf bifurcation.

To trace the evolution of the bifurcation points that appear in the above diagram (which we have called "wind steering diagram") we carried out codimension-2 continuation, starting from the turning point near beam wind at wind velocity $U_W = 24$ m/s. Wind velocity and rudder angle were then varied simultaneously. The obtained diagram is shown also in Fig. 3. As the wind is gradually lowered, one notes a secondary folding of the curve, generated at a cusp. Later on, the original folding disappears at a new cusp. These two cusps arise at wind velocities 19.8 m/s and 16.33 m/s. Therefore, in between the two cusps three turning points exist and thus an equal number of changes of stability take place. Codimension-2 continuation has been carried out also for the supercritical Hopf point that is responsible for the periodic yawing in head wind. The same was done for a new folding of the curve of equilibrium headings that is particular to the head wind region (Fig. 4). It is remarkable that these two curves coalesce at 25.65 m/s thus realising a so-called "Bogdanov-Takens" interaction phenomenon. Thereafter the branch of Hopf points seizes to exist which means that at very high wind speeds no self-sustained oscillations should be expected. A similar interaction is noted at very low wind speed as the Hopf curve moves nearer to the beam-wind condition, ultimately touching the locus of saddle nodes that exist in that region.

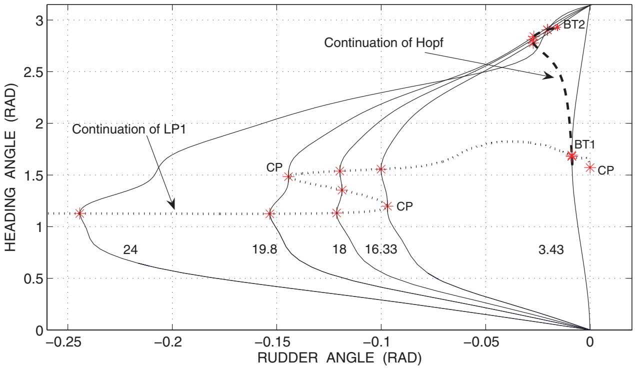

Fig. 3. Continuation of equilibrium headings and bifurcation loci

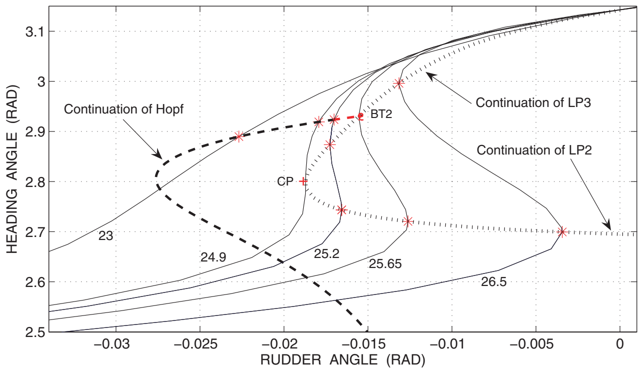

Fig. 4. As above, for the range of high wind velocities

3.2 Self-sustained Periodic Responses

By keeping a constant rudder angle δ = -0.020 rad, limit cycles emerged and died out smoothly from a supercritical Hopf point. This can be observed in Fig. 5 where 3-D view of the evolution of the limit-cycle is shown. It is notable that the amplitude droped after a certain wind velocity.

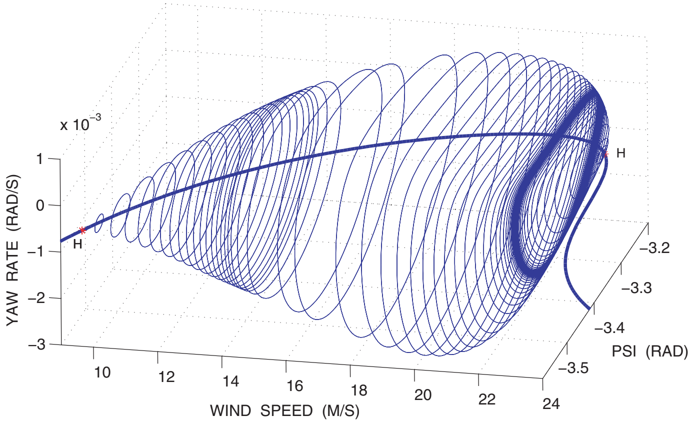

Fig. 5. 3-D view of periodic and stationary course-keeping states as wind speed is varied. (U_S = 6.18 m/s, δ = -0.020 rad)

A similar diagram, yielding though a different set of results, is shown in Fig. 6. In this case at a constant rudder angle of δ = -0.015 rad, limit cycles are again born from a supercritical Hopf point but they disappear abruptly as the wind velocity is increased. Simulation confirmed that the period of oscillation near that region increased to infinity. Superimposing the curve of equilibrium headings on the same graph revealed a homoclinic saddle connection. The oscillations change progressively in shape as they are drawn closer to the unstable stationary points. Ultimately, they disappear due to collision with an unstable equilibrium.

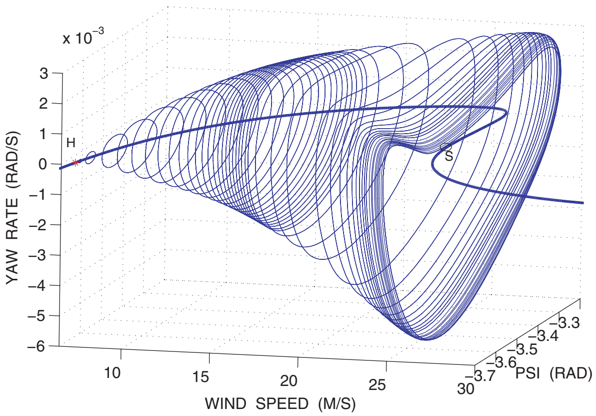

Fig. 6. 3-D view of periodic and stationary states as wind speed is varied (U_S = 6.18 m/s, δ = -0.015 rad)

4 Dynamic behaviour during turn

Setting the rudder at an angle should initiate turning motion. In unidirectional wind one expects that, for relatively small rudder angles, the motion after the initial transient will settle to one of the "course-keeping" patterns discussed in the previous section. For larger angles however the ship should be able to perform recurrent turns (which however should not "close" due to the directionality introduced to the field by the wind vector). These principal types of response are shown for two characteristic settings of the rudder in Fig. 7. It is conjectured that a bifurcation phenomenon determines the separatrix between the domains of course-keeping and turning, but its nature has not been identified thus far. We shall thus attempt to track the evolution of the periodic responses which correspond to turning motion. Unfortunately, continuation of periodic states cannot be performed directly upon the system of ordinary differential equations presented in Section 2 because, although a pattern of repetition is obtained, the variable that represents the heading ψ and appears explicitly in the state-vector of our system increases monotonically i.e. it is not a periodic function of time. In the first instance this poses a serious difficulty for performing continuation and to overcome this computational obstacle, some suitable transformation of the variable was contrived. Specifically, the following pair of dummy variables was introduced: $a = cos\psi$, $b = sin\psi$ under the condition $a^2 + b^2 = 1$. Then it is legitimate to substitute the kinematic relationship $\dot{\psi} = r$ that appears in the mathematical model by the pair of equations $\dot{a} = \frac{d}{dt}(\cos\psi) = -\dot{\psi}\sin\psi = -rb$, $\dot{b} = -ra$. By means of this transformation all variables of the modified state-vector are periodic functions and thus, in principle, it becomes feasible to carry out continuation of the steady turning motion pattern in wind, as the rudder angle is varied.

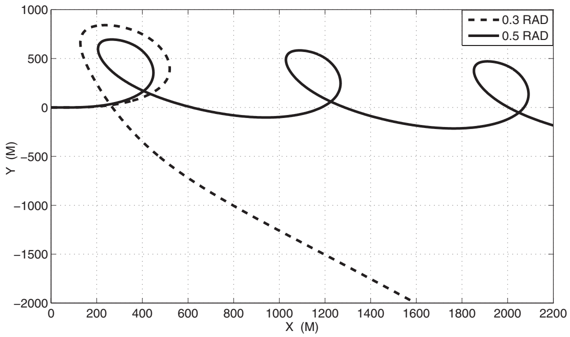

Fig. 7. Simulation of turn and course-keeping after change of rudder angle from 0.5 to 0.3 rad ($U_W = 26$ m/s and $U_S = 6.18$ m/s)

To initialize continuation, a periodic steady-state was captured by setting the rudder to maximum deflection. Then, by using a point of it as initial condition and progressively decreasing the rudder angle, the period of oscillation was traced going to infinity as a rudder angle about 0.30 rad was approached from higher values (Fig. 8). The character of the response pattern is grasped by the time-histories of the steady yaw rate shown in Fig. 9. It seems therefore that a homoclinic event must be taking place.

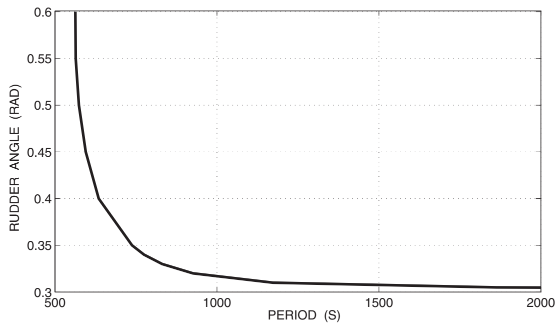

Fig. 8. The period of oscillation going to infinity ($U_W = 26$ m/s and $U_S = 6.18$ m/s)

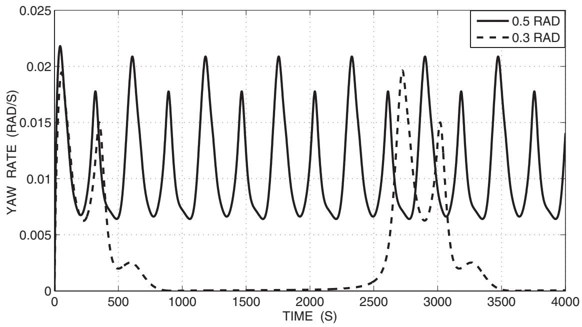

Fig. 9. Characteristic time histories of yaw rate in 0.304 and 0.5 rad ($U_W = 20$ m/s and $U_S = 6.18$ m/s)

In order to disclose the type of interaction that takes place, we have combined the current continuation of “turns” with the continuation of equilibrium headings as the rudder angle is varied. Thus, stationary behaviour associated with course-keeping and periodic behaviour realised during turning motion are shown in unison. The result is illustrated in the 3-D diagram of Fig. 10 which includes also the locus of saddle nodes (near beam wind) that appear in the curves of equilibrium headings. This particular curve was obtained through codimension-2 continuation, by considering both wind velocity and rudder

angle as control parameters.
The diagram reveals that a periodic state touches the curve of equilibria at a saddle-node of the latter. This is a special type of homoclinic bifurcation usually referred to as homoclinic-to-saddle-node or else omega-explosion. In this global bifurcation an intermittency catastrophe of the flow associated with the limit-cycles is realised. Below the critical rudder angle the limit cycle is broken and the trajectory spirals towards a nearby stable stationary heading. This trajectory (obtained by simulation) denotes clearly that the ship is unable to execute a complete turn, ending up on straight-line course.

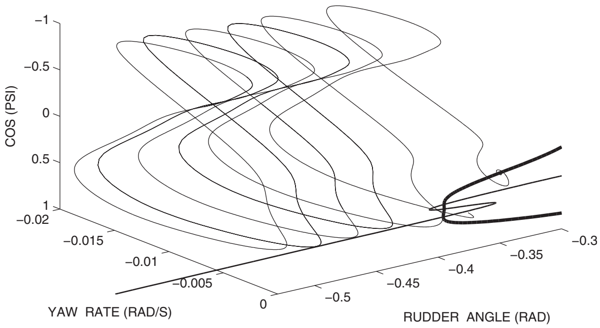

Fig. 10. A 3-D view of the periodic and stationary states as rudder angle is varied. The locus of saddle-nodes for a range of wind velocities is also shown. An omega explosion event is noted for $U_W = 28$ m/s and $U_S = 6.18$ m/s

We have checked whether the omega explosion could be globally identified as responsible for the destruction of the periodic states, for all wind velocities. It was observed that at a lower wind velocity ($U_W = 26$ m/s), omega explosion exchanges its place to a standard homoclinic saddle connection. This is verified by Fig. 11. At a much lower wind velocity however ($U_W = 16$ m/s) the phenomenon of omega explosion takes place again (Fig. 12). Therefore, the dynamical interaction phenomena, together with their domain in terms of wind velocity, that govern the separatrix between course-keeping and turning are summarised in Table 1. The three critical interactions discussed have been collected in a single diagram in Fig. 13.

5 Conclusion

For the investigated ferry the “course-keeping” and “turning” types of response in uniform wind are determined, for the most part of the realistic wind velocity range, by a homoclinic-to-saddle-node bifurcation. In the remaining cases the two are separated by a classical homoclinic saddle connection.

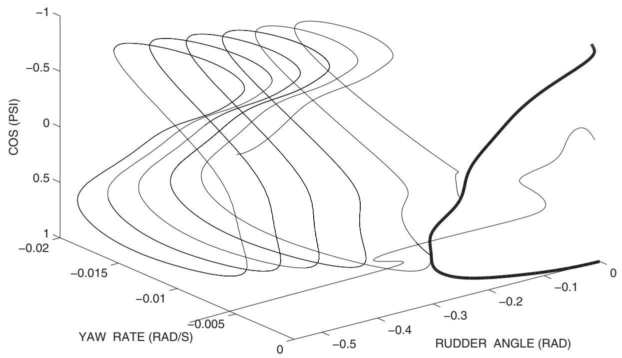

Fig. 11. As above, for $U_W = 26$ m/s and $U_S = 6.18$ m/s. A homoclinic saddle connection takes place

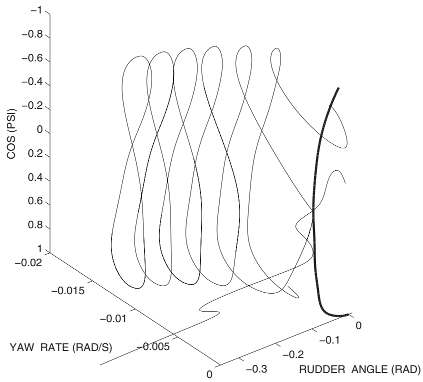

Fig. 12. As above, for $U_W = 16$ m/s and $U_S = 6.18$ m/s. The omega explosion has recurred

Table 1. Type of bifurcation per range of wind velocities

Wind velocity	Type of global bifurcation
until 17 m/s	Homoclinic-to-Saddle-Node
17 m/s to 28 m/s	Homoclinic-to-Hyperbolic-Saddle
above 28 m/s	Homoclinic-to-Saddle-Node

Acknowledgments

Ioannis Tigkas would like to thank “Alexander S. Onassis” Public Benefit Foundation for his PhD scholarship.

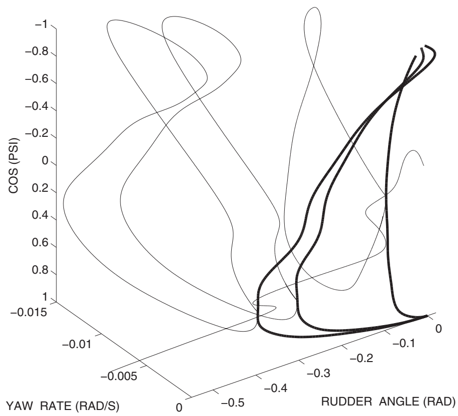

Fig. 13. Summary of critical interactions at three different wind velocities. ($U_W =$ 28 m/s, 26 m/s, 16 m/s and $U_S = 6.18$ m/s)

References

1. Euler L (1773) Theorie complette de la construction et de la manoeuvre des vaisseaux. Troisieme Partie. De la mâture et de la manoeuvre des vaisseaux, St. Petersbourg, Impr. Acad. Imperiale des Sciences, 153–268 (in French)
2. Eda H (1968) Journal of Ship Research 12:181–199
3. Ogawa A (1969) Journal of the Society of Naval Architects of Japan 126:117–120 (in Japanese)
4. Martin LL (1980) Transactions of the Society of Naval Architects and Marine Engineers 88:257–281
5. Asai S (1981) Journal of the Society of Naval Architects of Japan 150:245–253
6. Yoshimura Y, Nagashima J (1985) Journal of the Society of Naval Architects of Japan 158:125–136 (in Japanese)
7. Spyrou KJ (1995) Ship Technology Research/ Schiffstechnik 42:21–30
8. Spyrou KJ, Tigkas I, Chatzis A (2007) Journal of Ship Research 51(2):160–173
9. Dhooge A, Govaerts W, Kuznetsov YuA, Mestrom W, Riet AM, Sautois B (2003) MATCONT and CL-MATCONT: Continuation toolboxes for MATLAB, Report of Gent (Belgium) and Utrecht (Netherlands) Universities
10. Mikelis N (1985) In: Banda P, Kuo C (eds) Proceedings of International Conference of Shipyard Operation and Ship Design (ICCAS). Elsevier Publishers B.V., North Holland, 437–446
11. Blendermann W (1995) Proceedings of OMAE, Offshore Technology I-A:271–277
12. Blendermann W (1996) Wind loading of ships-collected data from wind tunnel tests in uniform flow, Report No.574, Shipbuilding Institute, University of Hamburg, Germany

Nomenclature

a_H	: rudder-to-hull interaction coefficient
A_F, A_L	: frontal, lateral windage area
A_R	: rudder area
C_X, C_Y, C_N, C_K	: wind loading coefficients in surge, sway, yaw, roll
f_Λ	: open-water normal rudder force coefficient
F_N	: rudder normal force
H	: max ship height
$\overline{H}$	: mean ship height
I_{xx}, I_{zz}	: roll, yaw ship mass moment of inertia
K_H, K_P, K_R, K_W	: hydrodynamic reaction, propeller, rudder and wind moments in roll
L_{OA}	: ship length overall
m	: ship mass
N_H, N_P, N_R, N_W	: hydrodynamic reaction, propeller, rudder and wind moments in yaw
p	: roll angular velocity
q_h	: dynamic pressure at reference height h
q_{ref}	: effective dynamic pressure
r	: yaw rate
u, v	: surge, sway velocity
U_R	: inflow velocity at rudder
U_S	: nominal ship speed
x_H	: x-coordinate of point of action of rudder to hull interaction force
X_H, X_P, X_R, X_W	: hydrodynamic reaction, propeller, rudder and wind forces in surge
z_R, x_R	: longitudinal, vertical position of rudder
Y_H, Y_P, Y_R, Y_W	: hydrodynamic reaction, propeller, rudder and wind forces in sway

Greek letters

δ	: rudder angle
Λ	: rudder aspect ratio
ρ	: water density
ϕ	: roll angle
ψ	: heading of ship